H_2SO_4 vapor and related compounds could permit a quantitative interpretation of the Venus spectrum, and is strongly encouraged. The near-surface association of CO_2 and water vapor is a direct result of our acceptance of the data of Terlouw *et al.* (*9*). It is critically important that the equilibrium behavior of this system be confirmed by further experiments. One can also directly test this model by using Venus water profiles to be measured by the Near Infrared Mapping Spectrometer experiment on the Galileo spacecraft (*16*). Further, the conditions of temperature and pressure and the high CO_2 and water vapor abundances conducive to extensive gaseous H_2CO_3 formation are closely similar to those hypothesized for early Earth. An improved understanding of the thermochemical and optical properties of this species may permit substantial improvement of these models.

REFERENCES AND NOTES

1. U. von Zahn, S. Kumar, H. Niemann, R. Prinn, in *Venus*, D. M. Hunten, L. Colin, T. M. Donahue, V. I. Moroz, Eds. (Univ. of Arizona Press, Tucson, 1983), pp. 299–430.
2. V. I. Oyama *et al.*, *J. Geophys. Res.* **85**, 7891 (1980).
3. H. E. Revercomb, L. A. Sromovsky, V. E. Suomi, *Icarus* **61**, 521 (1985).
4. V. I. Moroz, N. A. Parfent'ev, N. F. San'ko, *Cosmic Res. (U.S.S.R.)* **17**, 601 (1979).
5. L. D. G. Young, A. T. Young, L. V. Zasova, *Icarus* **60**, 138 (1984).
6. J. I. Gmitro and T. Vermeulen, *Am. Inst. Chem. Eng. J.* **10**, 740 (1964).
7. G. P. Ayers, R. W. Gillett, J. L. Gras, *Geophys. Res. Lett.* **7**, 433 (1980).
8. P. G. Steffes, *Icarus* **64**, 576 (1985).
9. J. K. Terlouw, C. B. Lebrilla, H. Schwartz, *Angew. Chem. Int. Ed. Engl.* **26**, 354 (1987).
10. Terlouw *et al.* (*9*) found in the mass spectrum of NH_4HCO_3 vapor (at 120 K) a peak for H_2CO_3 with a peak area somewhat less than 1% of that for CO_2. Vapor pressure data on NH_4HCO_3 (*17*) give a Gibbs free energy of vaporization to NH_3, H_2O, and CO_2 of -4600 cal mol^{-1} at 120 K. Because of the very large theoretical activation energy of at least 40 kcal mol^{-1} for dissociation of gaseous H_2CO_3 into water vapor and CO_2 (*18*), we assume that the CO_2:H_2CO_3 ratio was fixed at about 5×10^{-3} in the evaporation chamber rather than in the mass spectrometer. In combination with a ΔH^0_{298} of -146.1 kcal mol^{-1} for formation of H_2CO_3 from the elements (*9*) and a ΔH^0_{400} of -152.1 kcal mol^{-1} for gaseous CO_2 plus H_2O from the JANAF tables (*19*), we deduce an enthalpy change at 400 K of 6 kcal mol^{-1} and an entropy change of 2 cal mol^{-1} K^{-1} for reaction 2.
11. As a sensitivity test, we calculated a large number of models without using laboratory thermodynamic data on H_2CO_3 and H_2SO_4 vapors. Instead, grids of enthalpy and entropy values for both reactions were systematically explored to see which values could give a satisfactory fit to the Venus water profile. We found that the ranges of best-fit thermodynamic properties required to fit the Venus observations were extremely close to the published laboratory data.
12. V. G. Istomin, K. V. Grechev, V. A. Kochnev, *Space Res.* **20**, 215 (1980).
13. B. G. Gel'man *et al.*, *ibid.*, p. 219.
14. J. H. Hoffman, R. R. Hodges, Jr., T. M. Donahue, M. B. McElroy, *J. Geophys. Res.* **85**, 7882 (1980).
15. T. M. Donahue, personal communications.
16. J. B. Pollack, personal communication.
17. W. K. Hutchison, *J. Chem. Soc.* **1931**, 410 (1931); T. Stobiecki, A. Baranski, Z. Kowalski, *Chem. Stosow.* **1**, 81 (1957).
18. See, for example, M. T. Nguyen and T.-K. Ha, *J. Am. Chem. Soc.* **106**, 599 (1984).
19. *JANAF* (Joint Army-Navy-Air Force) *Thermochemical Tables* (Dow Chemical Company, Midland, MI, 1973).
20. L. W. Esposito, R. G. Knollenberg, M. Ya. Marov, O. B. Toon, R. P. Turco, in *Venus*, D. M. Hunten, L. Colin, T. M. Donahue, V. I. Moroz, Eds. (Univ. of Arizona Press, Tucson, 1983), pp. 484–564.
21. We thank K. Vemulapalli, D. M. Hunten, A. T. Young, and J. Kasting for helpful discussions.

4 December 1989; accepted 16 May 1990

Negative Pressure-Temperature Slopes for Reactions Forming $MgSiO_3$ Perovskite from Calorimetry

E. ITO, M. AKAOGI, L. TOPOR, A. NAVROTSKY

A new and sensitive differential drop solution calorimetric technique was developed for very small samples. A single experiment using one 5.18-milligram sample of perovskite, synthesized at 25 gigapascals and 1873 Kelvin, gave 110.1 ± 4.1 kilojoules per mole for the enthalpy of the ilmenite-perovskite transition in $MgSiO_3$. The thermodynamics of the reaction of $MgSiO_3$ (ilmenite) to $MgSiO_3$ (perovskite) and of Mg_2SiO_4 (spinel) to $MgSiO_3$ (perovskite) and MgO (periclase) were assessed. Despite uncertainties in heat capacity and molar volume at high pressure and temperature, both reactions clearly have negative pressure-temperature slopes, -0.005 ± 0.002 and -0.004 ± 0.002 gigapascals per Kelvin, respectively. The latter may be insufficiently negative to preclude whole-mantle convection.

$MgSiO_3$-RICH PEROVSKITE IS thought to dominate the earth's lower mantle (*1*). Knowing its stability is crucial for understanding the seismic discontinuity near 650 km and for predicting lower mantle properties. The pressure-temperature (P-T) slope (dP/dT) of reactions forming perovskite may help determine whether the mantle is compositionally layered or whether whole mantle convection can occur; a strongly negative slope would inhibit convection across the boundary (*2, 3*). The nature of convection has important implications for the evolution of the earth, its heat budget, and the coupling of convection in the core to processes in the mantle and crust.

Ito and Yamada (*4*) first demonstrated that for the transformations of $MgSiO_3$ ilmenite to perovskite and of Mg_2SiO_4 spinel to perovskite and periclase, have negative slopes ($dP/dT < 0$) and that both reactions occur at similar pressures and temperatures. Ito and Takahashi (*5*) refined these observations. They concluded that the pronounced sharpness of the 650-km discontinuity can be reasonably interpreted as the dissociation of silicate spinel into perovskite plus magnesiowustite. Although their data suggest that dP/dT is negative, pressure and temperature determinations in multianvil devices still have considerable uncertainties, and phase boundary reversals are difficult. Thus, the slope of the perovskite-forming reaction has remained somewhat uncertain. Because of the importance of this slope in considerations of whole mantle convection, it is desirable to determine dP/dT by a different and independent method, in order to test whether the phase synthesis runs were indeed close to equilibrium, to confirm that the slope is negative, and to obtain a reliable value for dP/dT.

High-temperature oxide melt solution calorimetry (*6*) offers a means of obtaining thermochemical data for high-pressure silicates (*7–9*). However, in order to apply this technique to the very small amounts of $MgSiO_3$ perovskite obtainable by synthesis at 25 GPa in a multianvil apparatus, its sensitivity had to be improved. In this report, we describe a new differential drop-solution technique and report a calorimetric determination, using 5 mg of perovskite, of the enthalpy difference between $MgSiO_3$ pyroxene and perovskite. Combination with earlier thermodynamic data (*7–10*) allows calculation of the stability fields of $MgSiO_3$ perovskite and comparison with high-pressure studies.

E. Ito, Institute for Study of the Earth's Interior, Okayama University, Misasa, Tottoriken, 682-02, Japan.
M. Akaogi, Department of Chemistry, Gakushuin University, Tokyo 171, Japan.
L. Topor and A. Navrotsky, Department of Geological and Geophysical Sciences, Princeton University, Princeton, NJ 08544.

Table 1. Enthalpy measured by differential drop solution calorimetry (sum of heat content, $H_{975} - H_{294}$, and heat of solution at 975 K).

Weight (mg)	Enthalpy (kJ mol^{-1})
$MgSiO_3$ orthopyroxene	
8.91	107.89
7.54	112.44
6.01	114.21
5.20	110.44
10.29	112.76
5.10	105.35
Average	110.52 ± 2.74*
$MgSiO_3$ perovskite	
5.18	0.38 ± 3†

*2 SD of mean. †Error estimated.

We pulverized stoichiometric, flux-grown $MgSiO_3$ (orthopyroxene) crystals (*11*) for calorimetry and perovskite synthesis. Perovskite was synthesized at 25 GPa and 1873 K in a uniaxial split-sphere apparatus (*4*) with cubic tungsten carbide anvils (3-mm truncation). Analysis of the run product with microfocused x-ray diffraction showed that the high-temperature central region of the product was perovskite. The lower temperature margins, consisting of ilmenite, were removed, and the perovskite was pulverized. Optically, >95% of the sample appeared homogeneous with index of refraction greater than 1.7. We detected only perovskite with conventional diffractometry.

A Calvet-type twin microcalorimeter (*6*) at 975 K was used for reaction calorimetry in molten $2PbO \cdot B_2O_3$. The small amount of perovskite and its easy decomposition on heating at atmospheric pressure presented special challenges. Direct high-temperature solution calorimetry (*6*), in which the sample must equilibrate at 975 K, was unsuitable. Transposed-temperature drop calorimetry (*6*) (in which the sample is dropped from room temperature into a high-temperature calorimeter with no solvent present), was inapplicable because decomposition products were poorly defined. Drop-solution calorimetry (*7*) (in which the sample is dropped from room temperature into molten lead borate), appeared possible. However, the small enthalpy associated with a sample drop would be swamped by large effects from the capsule and as a result the sensitivity would be poor.

We therefore devised a very sensitive differential drop solution technique. Two capsules of similar weights made of $2PbO \cdot B_2O_3$ glass (same as the solvent), one containing the sample and the other empty, were dropped simultaneously on opposite sides of the twin calorimeter into the melt. This method has several advantages over earlier drop solution calorimetry, which used capsules of platinum or pyrex glass (*7*). The lead borate capsules soften quickly and become part of the solvent. This brings the sample into intimate contact with solvent; thus, stirring is unnecessary. The only heat effect associated with the capsules is that small part of the enthalpy, $H_{975} - H_{294}$, not canceled between left and right sides arising from small differences in capsule weight (<0.5 mg) and in calibration factor (<0.5%). This effect can be determined accurately with the use of paired empty capsules of differing weights. The differential method yields enthalpies of drop solution (sum of heat content and enthalpy of solution) on 5- to 10-mg samples of $MgSiO_3$ (pyroxene) with precision and accuracy comparable to that obtained previously for 15- to 30-mg samples (*7*). We performed six experiments on pyroxene and one on perovskite (Table 1). Uncertainty in the perovskite runs is estimated comparable to that in the pyroxene run (±3 kJ mol^{-1}) (*12*). For perovskite, the observed heat effect (endothermic heat content plus exothermic heat of solution) is nearly zero. Direct measurement by the differential method is indeed the only approach having the necessary sensitivity.

The calorimetric data indicate that, for the reaction

$$MgSiO_3\ \text{(pyroxene)} = MgSiO_3\ \text{(perovskite)} \qquad (1)$$

the enthalpy change at room temperature and atmospheric pressure, ΔH^0_{294}, is

$$\Delta H^0_{294} (= \Delta H^0_{298}) = 110.52 - 0.38 = 110.1 \pm 4.1\ \text{kJ mol}^{-1}$$

Thermochemical cycles with recent calorimetric data for ilmenite and spinel (*7–10*) provide enthalpies for (Table 2)

$$MgSiO_3\ \text{(ilmenite)} = MgSiO_3\ \text{(perovskite)} \qquad (2)$$

$$\Delta H^0_{298} = 51.1 \pm 6.6\ \text{kJ mol}^{-1}$$

and

$$\underset{\text{(spinel)}}{Mg_2SiO_4} = \underset{\text{(perovskite)}}{MgSiO_3} + \underset{\text{(periclase)}}{MgO} \qquad (3)$$

$$\Delta H^0_{298} = 96.8 \pm 5.8\ \text{kJ mol}^{-1}$$

These enthalpy values, based on direct calorimetric determination, refine the esti-

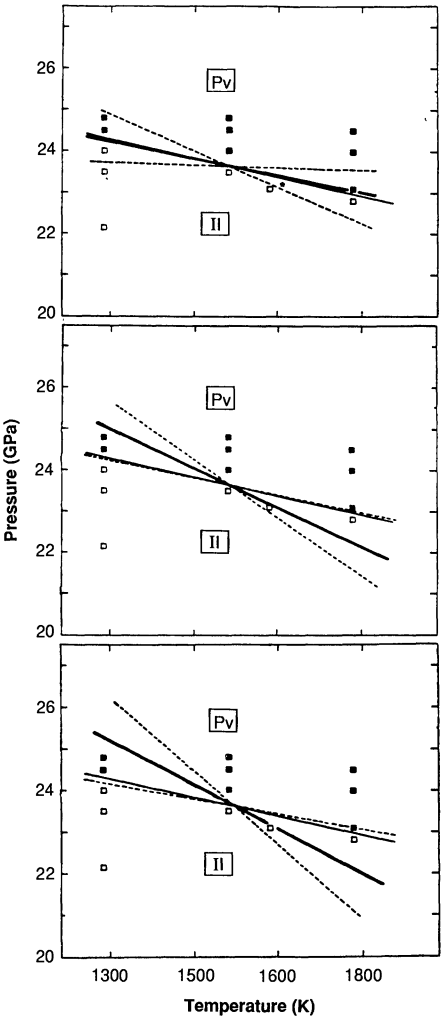

Fig. 1. Calculated phase boundaries (bold lines) compared to experimental data (*5*) (thin solid lines) for the reaction $MgSiO_3$ (ilmenite) = $MgSiO_3$ (perovskite). Squares are experimental data points; open are low-pressure assemblage; solid are high-pressure assemblage. (**Top**) "Simple" calculation with constant ΔV; (**middle**) corrected calculation, $\alpha = 2.2 \times 10^{-5}$ K^{-1}; (**bottom**) corrected calculation, $\alpha = 4 \times 10^{-5}$ K^{-1}. Dashed lines represent uncertainty from errors in ΔH^0. Il is ilmenite; Pv is perovskite.

Table 2. Thermochemical cycles used in phase boundary calculations for $MgSiO_3$ and Mg_2SiO_4 (SOL is dilute solution in $2PbO \cdot B_2O_3$; Px is pyroxene; Pv is perovskite; Il is ilmenite; Per is periclase; Ol is olivine; Sp is spinel).

Reaction	ΔH^0 (kJ mol^{-1})	ΔS^0 (J K^{-1} mol^{-1})	ΔV^0 (cm^3 mol^{-1})
Px (295 K) = SOL (975 K)	110.5 ± 2.7		
Pv (295 K) = SOL (975 K)	0.4 ± 3.0		
Il = Pv	51.10 ± 6.60	Table 4	−1.89 (*4*)
Ol = Px + Per	27.72 ± 1.19 (*10*)	−0.39 ± 0.95 (*10*)	−1.10 (*24*)
Ol = Sp	39.05 ± 2.62 (*8*)	−5.0 ± 2.4 (*8*)	−4.14 (*8*)
Px = Il	59.03 ± 4.26 (*7*)	−15.5 (*7*)	−4.94 (*7*)
Sp = Pv + Per	96.80 ± 5.8	Table 4	−3.79 (*4*)

mates given previously (*13, 14*), which were based on phase synthesis studies of perovskite.

The phase boundary is the locus of points where $\Delta G(T,P) = 0$ (*15*).

$$\Delta G(T,P) = \Delta H^0(T) - T\Delta S^0(T) + \int_{1\ \mathrm{atm}}^{P} \Delta V(P,T)\mathrm{d}P = 0 \qquad (4)$$

Temperature dependences of ΔH^0 and ΔS^0 arise from differences in heat capacities between products and reactants, ΔC_p. Because ΔH^0 is large, the effect of $\int \Delta C_p\, dT$ is relatively small but ill-constrained because of lack of heat capacity data for perovskite. Although estimates of the perovskite heat capacity have been made through vibrational modeling and internally consistent data bases (*13*), their accuracy is hard to judge. Any uncertainties in the thermal expansivity of perovskite also affect theoretical C_p values. From 298 to 2000 K, the assumption that ΔH^0 is constant ($\Delta C_p = 0$) is reasonable.

Phase equilibrium calculations may be done at two levels of complexity. In the simple calculation $\Delta V(P,T)$ is assumed to be constant and equal to ΔV^0_{298}. This assumption does not bias the calculation by arbitrary choice of equation of state. The corrected calculation incorporates the effects of compression and thermal expansion (*7–9*). Although more accurate in principle, it is sensitive to uncertainties in compressibilities and expansivities and to the form of $V(P,T)$. Although the bulk moduli (K) and their temperature derivatives (K') are fairly well constrained at room temperature (*16–20*), both for perovskite and the lower pressure phases, there is some uncertainty in the thermal expansivity, α, of the perovskite (*21–23*). To illustrate the effects of these uncertainties on the calculated phase boundaries, we describe three calculations: (i) simple, $\Delta V(P,T)$ = constant, (ii) corrected, $\alpha = 2.2 \times 10^{-5}$ K^{-1}, and (iii) corrected, $\alpha = 4 \times 10^{-5}$ K^{-1} (Tables 3 and 4).

Were ΔS^0_{298} known for reactions 2 and 3, phase equilibrium calculations completely independent of high P-T experiments could be made. Standard entropies are not available for perovskite, and we proceed as we have previously (*7–9*), by choosing one point on the experimental phase diagram to constrain $\Delta G^0(T)$ and, knowing ΔH^0 and $\Delta V(P,T)$, calculating ΔS^0 and the boundary (Tables 3 and 4). For reaction 2, this point is 23.5 GPa, 1573 K (*5*), representing a fairly tight reversal. For reaction 3 it is 24.0 GPa, 1573 K (*5*). For all three calculations, entropies of both perovskite-forming reactions are positive and slopes slightly but definitely negative (Figs. 1 and 2). Including compression and thermal expansion accentuates this result. Larger α makes ΔS^0 more positive. The P-T slopes for both reactions remain definitely negative after including the uncertainty in ΔH^0 (dashed lines in Figs. 1 and 2). The slopes also remain negative for reasonable variations in the bulk moduli used. These results confirm the high P-T experiments (*4, 5*). Our best estimates of the slopes are −0.005 ± 0.002 GPa K^{-1} for reaction 2 and −0.004 ± 0.002 GPa K^{-1} for reaction 3.

Table 3. Bulk moduli (K_0), their assumed pressure derivatives (K'), and thermal expansivities (α).

Phase	K_0 (GPa)	K'_0	α (10^5 K^{-1})
Mg_2SiO_4 (Ol)	184 (16)	4	2.6 (*20*)
Mg_2SiO_4 (Sp)	212 (17)	4	2.4 (*20*)
$MgSiO_3$ (Pv)	246 (18)	4	2.2 (*21*), 4 (*22*)
MgO (Per)	163 (19)	4	4.2 (*25*)

Table 4. Calculated entropy changes and P-T slopes.

Parameter	Simple	Corrected $\alpha = 2.2 \times 10^{-5}$ K^{-1}	Corrected $\alpha = 4 \times 10^{-5}$ K^{-1}
		Il = Pv (reaction 2)	
ΔS^0 (J K^{-1} mol^{-1})	4.2 ± 4.0	5.7 ± 4.2	13.8 ± 4.2
dP/dT (GPa K^{-1})	−0.002 ± 0.002	−0.005 ± 0.003	−0.006 ± 0.004
		Sp = Pv + Per (reaction 3)	
ΔS^0 (J K^{-1} mol^{-1})	3.7 ± 3.6	11.1 ± 3.7	19.3 ± 3.7
dP/dT (GPa K^{-1})	−0.001 ± 0.001	−0.004 ± 0.002	−0.004 ± 0.002

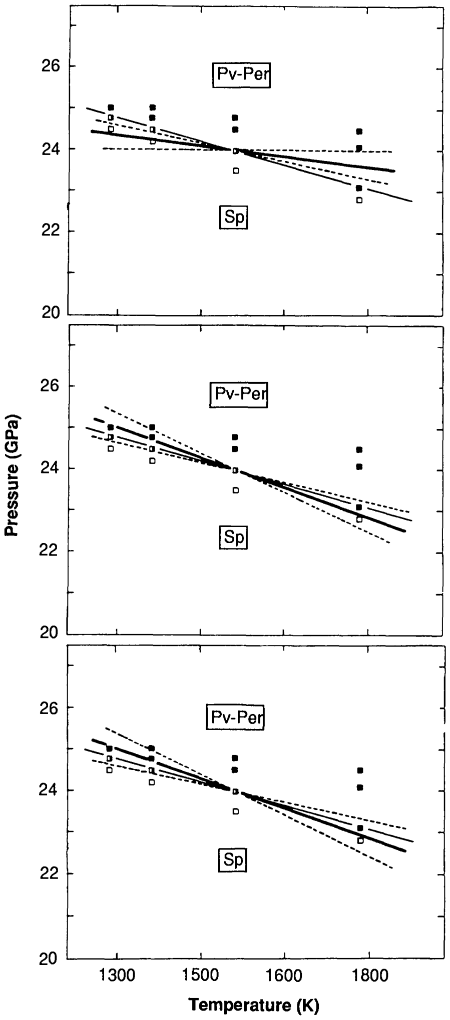

Fig. 2. Phase boundaries for the reaction Mg_2SiO_4 (spinel) = $MgSiO_3$ (perovskite) + MgO (periclase). Labeling as in Fig. 1. Sp is spinel; Pv is perovskite; Per is periclase.

In a periodotitic mantle, dissociation of silicate spinel causes the 650 km discontinuity (*1, 5*). A recent numerical analysis of dynamic mantle motion (*3*) suggests that dP/dT must be more negative than −0.006 GPa K^{-1} to completely inhibit convection. Our analysis suggests a slope of similar but somewhat smaller magnitude (−0.004 ± 0.002 GPa K^{-1}). Thus whole mantle convection may not be ruled out by the thermochemical properties of $MgSiO_3$ perovskite. However, this conclusion is sensitive to uncertainties in the numerical analysis of convection, as well as to the effects of other constituents (Fe, Ca, Al) on the phase boundary slopes. In any case, the calculated slope is likely to remain close to the critical value, perhaps exceeding it in some parts of the mantle but not in others. We suggest that local heterogeneity at the 650-km discontinuity may govern the extent of convection in a particular region.

REFERENCES AND NOTES

1. I. Jackson, *Earth Planet Sci. Lett.* **62**, 91 (1983); E. Ito, E. Takahashi, Y. Matsui, *ibid.* **67**, 238 (1984).
2. J. Verhoogen, *Philos. Trans. R. Soc. London Ser. A* **258**, 276 (1965).
3. U. Christensen and D. A. Yuen, *J. Geophys. Res.* **89**, 4389 (1984).
4. E. Ito and H. Yamada, in *High-Pressure Research in Geophysics*, S. Akimoto and M. H. Manghnani, Eds. (Terra Scientific, Tokyo, 1982), pp. 405–419.
5. E. Ito and E. Takahashi, *J. Geophys. Res.* **94**, 10,637 (1989).
6. A. Navrotsky, *Phys. Chem. Minerals* **2**, 89 (1977).
7. T. Ashida, S. Kume, E. Ito, A. Navrotsky, *Phys. Chem. Minerals* **16**, 239 (1988).
8. M. Akaogi, E. Ito, A. Navrotsky, *J. Geophys. Res.* **94**, 15,671 (1989).
9. A. Navrotsky, F. S. Pintchovski, S. Akimoto, *Phys. Earth Planet. Inter.* **19**, 275 (1979).

10. T. L. Charlu, R. C. Newton, O. J. Kleppa, *Geochim. Cosmochim. Acta* **39**, 1487 (1975).
11. H. Takei, S. Hosoya, M. Ozima, in *Materials Science of the Earth's Interior*, I. Sunagawa, Ed. (Terra Scientific, Tokyo, 1984), pp. 107–130.
12. It is obviously impossible to obtain any statistical measure of uncertainty based on one experiment. However, this run appeared normal in all respects, and it is reasonable to assume an uncertainty similar to that obtained for the pyroxene. Obtaining enough perovskite for the five to eight replicate runs needed for meaningful statistics is at present far too time-consuming and costly.
13. Y. Fei, S. K. Saxena, A. Navrotsky, *J. Geophys. Res.* **95**, 6915 (1990).
14. A. Navrotsky in *High-Pressure Research in Mineral Physics*, M. Manghnani and Y. Syono, Eds. (Terra Scientific, Tokyo, 1987), p. 261; *Prog. Solid State Chem.* **17**, 53 (1987); in *Perovskite—A Structure of Great Interest to Geophysics and Materials Science*, A. Navrotsky and D. J. Weidner, Eds. (American Geophysical Union, Washington, DC, 1989), pp. 67–80.
15. $\Delta G(T,P)$ is the Gibbs free energy of reaction at an arbitrary pressure and temperature (equal to zero along the phase boundary); $\Delta G^0(T)$, $\Delta H^0(T)$, and $\Delta S^0(T)$ are the Gibbs free energy, enthalpy, and entropy of reaction at one atmosphere and the given temperature. $DV(P,T)$ is the volume change for the reaction at a given pressure and temperature; $\Delta V^0 298$ is the volume change at ambient conditions. C_p is heat capacity and ΔC_p is the difference in heat capacity of products and reactants.
16. D. J. Weidner, H. Sawamoto, H. Sasaki, M. Kumazawa, *J. Geophys. Res.* **89**, 7852 (1984).
17. D. J. Weidner and E. Ito, *Phys. Earth Planet. Inter.* **40**, 65 (1985).
18. A. Yeganeh-Haeri, D. J. Weidner, E. Ito, *Science* **243**, 787 (1989).
19. Y. Sumino and O. L. Anderson, in *CRC Handbook of Physical Properties of Rocks*, R. C. Carmichael, Ed. (CRC Press, Boca Raton, FL, 1984), vol. 3, pp. 39–138.
20. I. Suzuki, E. Ohtani, M. Kumazawa, *J. Phys. Earth* **27**, 53 (1979).
21. N. L. Ross and R. M. Hazen, *Phys. Chem. Minerals* **16**, 415 (1989).
22. E. Knittle, R. Jeanloz, G. L. Smith, *Nature* **319**, 214 (1986).
23. The data of Ross and Hazen (*21*) ($\alpha = 2.2 \times 10^{-5}$ K^{-1}) refer to temperatures between 75 and 300 K, whereas those of (*22*) ($\alpha = 4 \times 10^{-5}$ K^{-1}) refer to temperatures between 300 and 850 K. Although a higher thermal expansivity at higher temperatures is generally expected because of increasing anharmonicity, decomposition of perovskite to glass or pyroxene complicates the higher temperature data, and the value of α at temperatures greater than 500 K is uncertain. Pressure may be expected to decrease thermal expansivity by suppressing anharmonicity. Possible phase transitions in the perovskite at high pressures p and t temperatures (from orthorhombic to tetragonal to cubic) may also affect α. Thus the thermal expansivity under mantle conditions is not well-constrained, and we examine the effect of these uncertainties by doing two sets of calculations using different constant values of α.
24. Joint Committee on Powder Diffraction Standards, International Center for Diffraction Data, Swarthmore, PA (1988), cards 4-829 and 34-189.
25. I. Suzuki, *J. Phys. Earth* **27**, 53 (1979).
26. We thank M. Ozima for providing the orthopyroxene sample. Supported by U.S. National Science Foundation and Japan Society for the Promotion of Science.

8 May 1990; accepted 23 July 1990

Direct Measurement of Forces Between Linear Polysaccharides Xanthan and Schizophyllan

DONALD C. RAU AND V. ADRIAN PARSEGIAN

Direct osmotic stress measurements have been made of forces between helices of xanthan, an industrially important charged polysaccharide. Exponentially decaying hydration forces, much like those already measured between lipid bilayer membranes or DNA double helices, dominate the interactions at close separation. Interactions between uncharged schizophyllans also show the same kind of hydration force seen between xanthans. In addition to the practical possibilities for modifying solution and suspension properties through recognition and control of molecular forces, there is now finally the opportunity for theorists to relate macroscopic properties of a polymer solution to the microscopic properties that underlie them.

POLYSACCHARIDES HAVE A CAPACITY to stabilize cellular or colloidal suspensions, an ability to maintain or even to facilitate bulk transport in muci and gels, and a high interaction specificity in cell recognition; they are used industrially to the extent of the millions of metric tons. The key to understanding these properties seems to be in understanding the physical interactions of these molecules with each other as well as with their aqueous environment. We now report direct measurements by the osmotic stress method (*1, 2*) of hydration forces between molecules of uncharged schizophyllan and of charged xanthan, both stiff linear polysaccharides.

These measurements offer an opportunity to relate directly measured molecular interactions to macroscopic solution properties. For example, we may now undertake an entirely new kind of investigation to relate the molecular basis of the hydrodynamic radius with the strength of perturbation of boundary water. Further, we can now expect to relate changes in forces with changes in solution viscosity, hygroscopic power, and gel-forming properties. This power might, in turn, lead to systematic design of better stabilizers of practical importance and provide the opportunity to relate directly measured interactions to the chemical identity of surfaces.

The most remarkable feature of this interaction occurs at surface separations of 2 to 10 Å where there is an exponentially varying force with a decay length of ~3.3 Å, totally unlike expectations from electrostatics, van der Waals interactions, or molecular packing entropies. This is very much like the "hydration force" seen, again by osmotic stress measurements, between electrically neutral or charged phospholipid bilayers (*3*) and between DNA double helices (*4, 5*) at comparable separations in many different ionic solutions. The observation of dominating hydration forces between these polysaccharides suggests an important role for these interactions in determining their function and properties.

Measured forces between xanthans show little dependence on the kind or concentration of salt. From a practical viewpoint, there is a remarkable correlation between the properties of this material seen by our measurements and the qualities that make it so valuable in food technology, oil recovery, and other industrial applications. The same molecular stiffness that imparts high solution viscosity causes mutual alignment at well-defined separation; the same hygroscopic power that stabilizes suspensions under all ionic conditions is seen as a hydration force insensitive to the kind and concentration of salt in the suspending medium.

Osmotic stress has been used in quantitative force measurement for at least 15 years, beginning with forces between phospholipid bilayer membranes (*1, 2*). Recently it has been developed to reveal both force and motion of DNA molecules as well as of membranes in thermodynamically well-defined assemblies (*5, 6*). This method is based on the ability of an "indifferent polymer" [for example, polyethylene glycol (PEG) or polyvinylpyrolidone (PVP) or dextran], to phase separate from many biopolymers, particularly stiff, hydrophilic macromolecules in aqueous solution. The osmotic pressure of the polymer in its phase exerts a force on the macromolecular phase that is balanced at equilibrium by the intermolecular repulsion between the biopolymers. Small ions and water are free to move between the two phases. Distances between macromolecules, equilibrated against a known PEG or PVP solution osmotic pressure and salt environment, are determined from the spacing of the interaxial reflections observed by x-ray

---

Laboratory of Biochemistry and Metabolism, National Institute of Diabetes and Digestive and Kidney Diseases, and Physical Sciences Laboratory, Division of Computer Research and Technology, Building 12A, Room 2007, National Institutes of Health, Bethesda, MD 20892.